Hydrodynamic Selection of the Kinetic Pathway of a Polymer Coil-Globule Transition

Kumiko Kamata, Takeaki Araki, and Hajime Tanaka[*]

Institute of Industrial Science, University of Tokyo, Meguro-ku, Tokyo 153-8505, Japan
(Received 16 January 2008; published 11 March 2009)

Recently, the role of hydrodynamic interactions in the selection of a kinetic pathway for phase transitions has attracted considerable attention. Here we study this problem numerically by taking as an example a coil-globule transition of a single polymer, which is a prototype model of protein folding. When a swollen polymer collapses into a globule state, hydrodynamic interactions accelerate the transition. We find, on the other hand, that when a rather compact polymer collapses into the same final state, hydrodynamic interactions decelerate the transition due to a slow squeezing process of the solvent. We reveal that the degree of the initial enhancement of anisotropy of the polymer configuration determines whether hydrodynamic interactions accelerate or decelerate the collapsing dynamics. We also discuss the possible relevance of squeezing flow effects in protein folding.

Hydrodynamic interactions (HIs) often change the kinetic pathway of ordering of soft matter. The most well-known example is phase separation of a binary liquid mixture. Unlike phase separation of a solid mixture, hydrodynamic transport of material makes a new coarsening mechanism active: Siggia's hydrodynamic pumping mechanism for bicontinuous phase separation [1]. The mechanism even leads to a domain coarsening law different from those for solids. In this case, we may say that the momentum conservation selects the kinetic pathway. It was also shown that phase separation of polymer solutions, protein solutions, and colloidal suspensions are strongly influenced by the momentum conservation law including viscoelastic effects [2].

In this way, any transitions occurring in a liquid may be strongly affected by HIs. For polymer dynamics, the difference between the Rouse and the Zimm model is known to arise from HIs [3]. Here we consider a coil-globule transition (CGT) of a polymer chain immersed in a liquid [4]. When the solvent quality is changed from "good" to "poor," e.g., by a temperature (T) decrease, a polymer chain collapses from a swollen to a compact globule state. The thermodynamic nature of CGT has been rather well understood [5]. Because of experimental difficulties, the effects of HIs on CGT has been discussed mainly theoretically [6,7], and by numerical simulations [8–12]. Despite these studies, the dynamics remains elusive due to the complex nature of HIs. Since the CGT is regarded as a prototype model of protein folding [13], this problem also has a biological significance with regards to understanding dynamic roles of a solvent (water) in the selection of the kinetic pathway of protein folding.

Following the pioneering works [6,8], this problem of hydrodynamic effects has recently been revisited by using state-of-the-art numerical simulations [9–12]. For example, Kikuchi *et al.* reported that HIs accelerate the CGT of a flexible polymer and also affect the morphology in the shrinking process [11]. Chang and Yethiraj also

proposed that HIs tend to prevent a collapsing polymer from being trapped at local energy minima [10]. These studies clearly showed acceleration effects of HIs.

Recently, Tanaka speculated that HIs not only accelerate the CGT, but also may retard it via a squeezing flow effect [14]. Note that HIs slow the dynamics of colloidal aggregation for certain configurations of particles since when particles of a finite volume are approaching each other the solvent between them has to be squeezed out [15]. In this Letter, we systematically study the dynamics and kinetic pathway of the CGT by comparing numerical simulations with and without hydrodynamics.

Treating polymers and a solvent on a microscopic level, e.g., by molecular dynamics simulations, is quite expensive computationally, and thus it is difficult to simulate the process of the CGT that typically occurs in a time scale of 1 ms. The long-range nature of hydrodynamics makes the situation worse. Thus, a proper coarse graining is necessary. Various numerical methods have been proposed and employed [8–12,16–18]. Here we explain our coarse-graining strategy. We express a polymer by a bead-spring model [3]. The novelty of our method comes from the usage of an undeformable spherical fluid particle as a bead. This method, which we call the fluid particle dynamics (FPD) method [15,19], was originally developed to study colloidal particles interacting via HIs without suffering from the solid-fluid boundary condition. It is a hybrid simulation method: the flow field is solved on a cubic lattice and the particle position is treated off lattice. In our polymer problem, a particle represents a blob. We describe particle i on the lattice as $\phi_i(\vec{r}) = [\tanh(a - |\vec{r} - \vec{r}_i|)/\xi + 1]/2$, where $\vec{r}$ is a lattice coordinate. $\vec{r}_i$, a, and ξ are the position vector of the center of mass, the particle radius, and the interfacial width, respectively. We introduce a Lennard-Jones (LJ) potential between particles $V_{LJ}(r) = 4\epsilon\{(2a/r)^{12} - (2a/r)^6\}$, where ϵ is the strength of the potential. A particle also interacts with the others via a harmonic potential: $V_{sp}(r) = \frac{1}{2}\kappa\sum_{i=1}^{N-1}(|\vec{r}_{i+1} - \vec{r}_i| - 2a)^2$,

where N is the number of particles and κ is the entropic spring constant. We set κ to be large enough for the spring length to be almost preserved around the particle diameter ($2a$) [20]. Thus, the polymer chain does not cross itself: it is "not" a phantom chain. The force acting on particle i is thus given by $\vec{F}_i = -(\partial/\partial\vec{r}_i)\sum_{j\neq i}^{N}\{V_{LJ}(r_{ij}) + V_{sp}(r_{ij})\}$ (here $r_{ij} = |\vec{r}_j - \vec{r}_i|$), which is mapped on the lattice as $\vec{F}(\vec{r}) = \sum_i^N \vec{F}_i \phi_i(\vec{r})/\int d\vec{r}\phi_i(\vec{r})$.

The gyration radius R_g of the polymer depends upon ϵ [see the inset of Fig. 4(b)]. We scaled the energy (e.g., ϵ) by k_BT (k_B is Boltzmann's constant). R_g is calculated as $R_g^2 = (1/N)\sum_{i=1}^{N}|\vec{r}_i - \vec{r}_c|^2$, where $\vec{r}_c$ is the position vector of the center of mass of the polymer chain. R_g becomes equal to R_g of the ideal chain, $R_g^\theta = a\sqrt{N/6}$, at θ point [3,4]. In this study, we quench the system from various initial states ($R_g = R_g^i$) to the common final state $\epsilon = 4.76$ ($R_g = R_g^f$). Even in this collapsed state, $R_g^f/R_g^\theta \approx 0.61$. This means that the polymer density in a particle is rather low even in the final collapsed state, which allows us to assume that the viscosity is homogeneous in space: $\eta(\vec{r}) = \eta$. This assumption of homogeneous viscosity and the absence of inertia effects extremely simplify our problem. Under the incompressible condition, the flow field $\vec{v}(\vec{r})$ is calculated from the Navier-Stokes equation, $\vec{F}(\vec{r}) - \vec{\nabla}p + \eta\nabla^2\vec{v} + \vec{\nabla}\cdot\overleftrightarrow{\sigma} = 0$, as $\vec{v}(\vec{r}) = \int \overleftrightarrow{T}(\vec{r} - \vec{r}')\cdot\{\vec{F}(\vec{r}') + \nabla\cdot\overleftrightarrow{\sigma}(\vec{r}')\}d\vec{r}'$, where $\overleftrightarrow{T}(\vec{r}) = \{\overleftrightarrow{I} + \vec{r}\vec{r}/r^2\}/(8\pi\eta r)$ is the Oseen tensor. Here $\overleftrightarrow{\sigma}$ represents thermal stress fluctuations satisfying the following fluctuation-dissipation theorem: $\langle\sigma^{\alpha\beta}(\vec{r}, t)\sigma^{\gamma\delta}(\vec{r}', t')\rangle = 2\eta(\delta_{\alpha\gamma}\delta_{\beta\delta} + \delta_{\beta\gamma}\delta_{\alpha\delta} - \frac{2}{3}\delta_{\alpha\beta}\delta_{\gamma\delta})\delta(\vec{r} - \vec{r}')\delta(t - t')$. Then, the position of the ith particle is updated by the averaged velocity inside the particle as $d\vec{r}_i/dt = \int d\vec{r}\, \vec{v}(\vec{r})\phi_i(\vec{r})/\int d\vec{r}\phi_i(\vec{r})$.

The space is discretized onto a lattice by using ξ as a unit and the time is scaled by $t_0 = \eta\xi^3/\epsilon$. We set $N = 50$, $a/\xi = 3$, and $\kappa a^2/\epsilon = 31.25$. We employ periodic boundary conditions on a cubic lattice (64^3) and a time increment $\Delta t = 0.01$. A typical unit time is $t_0 \approx 10$ ns for $a = 10$ nm, $\eta = 10^{-3}$ Pa, and $T = 300$ K. Typically we analyzed the processes of seven runs starting from exactly the same initial configuration, but with different noises, and took the average to reduce the statistical errors.

In order to elucidate roles of "many-body" HIs in CGT, we also perform Brownian dynamics (BD) simulations, where hydrodynamics is free draining and thus incorporate only "single-body" HIs. The roles of the solvent in BD are only to give thermal fluctuations and the "local" friction between a particle and the solvent. We solve the following Langevin equation for the overdamped limit (no inertia effects): $\zeta d\vec{r}/dt = \vec{F}_i + \vec{\xi}_i$, where ζ is the friction constant and $\vec{\xi}_i$ is the thermal noise satisfying $\langle\xi_i^\alpha(t)\xi_j^\beta(t')\rangle = 2\zeta\delta_{ij}\delta_{\alpha\beta}\delta(t - t')$. We set ζ such that the viscous friction of a single particle becomes the same between BD and FPD. We confirmed that the resulting particle diffusivities

of the two methods estimated from free diffusion coincide with each other within 5%.

First, we show results for a quench from a good (G) to a poor (P) solvent, i.e., for $R_g^i/R_g^\theta = 1.66$ [Fig. 1(a)]. We can see that HIs accelerate the collapsing process, as previously reported [11]. Typical snapshots of the configurations are also drawn in the inset. For BD polymer, clusters are formed around both ends of the polymer and grow with time by absorbing the slack polymer between them [21]. For FPD polymer, on the other hand, the polymer forms a sausagelike elongated structure [6], which then thickens and shortens with time and eventually collapses into a globule state. To see this difference more clearly, we characterize the shape of a polymer as follows: We average a polymer structure over $\Delta t = 10$ to remove the influence of thermal fluctuations, replace a bead by a Gaussian field $[\psi(\vec{r}) = \exp[(|\vec{r}_i - \vec{r}|/10)^2]]$, extract the shape of the polymer by setting the interface at $\psi(\vec{r}) = 2.0$, and calculate the Gaussian curvature K of the interface. Figure 2(a) shows that the FPD polymer transiently has a sausagelike shape, which is composed of the cylindrical part ($K = 0$) and the end caps ($K > 0$). On the other hand, the BD polymer has a saddle-shaped ($K < 0$) part, reflecting the cluster formation at both ends. For a longer chain ($N = 80$), we observe the similar tendency. However, the degree of hydrodynamic delocalization of the clusters formed at the chain ends becomes weaker (less sausagelike) for a chain of larger N.

Figure 1(c) shows results for a quench from a slightly poor (SP) to poor (P) solvent, i.e., for $R_g^i/R_g^\theta = 0.81$. There is little difference in the morphological change between BD and FPD. For both cases, the polymer shrinks with time while keeping a rather spherical configuration. Interest-
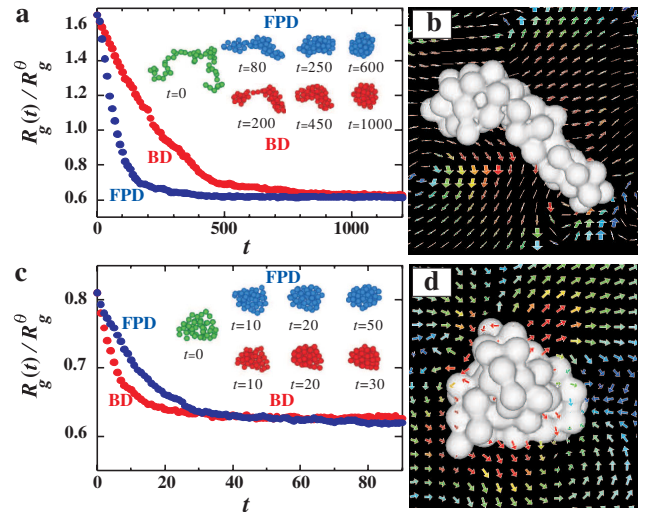

FIG. 1 (color online). Temporal change of R_g/R_g^θ for a G-to-P (a) and a SP-to-P quench (c). Insets depict the CGT processes. Flow fields around the FPD polymer are shown in (b) and (d) for quenches (a) and (c), respectively. The darker (red) the arrow color, the stronger the flow.
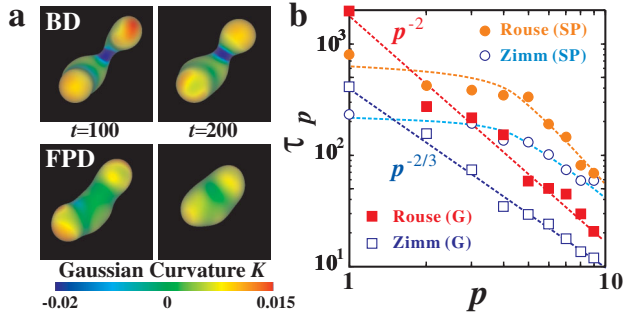
FIG. 2 (color online). (a) Comparison of polymer shapes at $t = 100$ and 200 for BD and FPD. The surface color represents the Gaussian curvature K (see the color bar). (b) Dependence of the relaxation time of mode p, τ_p, on the mode number p for BD and FPD polymers. The straight lines have slopes of -2 and $-2/3$, consistent with predictions of Rouse and Zimm models, respectively. The curves are to guide the eye.

ingly, HIs decelerate the collapsing process in this case. Figure 1(d) shows that there is flow of the solvent squeezed out from the inside of the polymer along the radial directions. We claim that the nonlocal viscous friction is the origin of deceleration of the CGT.

It is well known that HIs drastically accelerate polymer dynamics: Rouse versus Zimm model [3,16]. As shown in Fig. 2(b), the normal-mode analysis shows that $\tau_{p=1}$ at equilibrium is shorter by a factor of ~ 5 and 3–4 for FPD than for BD, respectively, for the two initial states, G and SP in Fig. 1. The mode number (p) dependence of τ_p is consistent with the theories for a swollen polymer, but not for a compact polymer where the theories lose their validity due to the presence of intersegment attractive interactions and a finite segment volume. The acceleration due to HIs for the collapsing from the swollen G state is nearly a factor of 4 [Fig. 1(a)], which is about the same as the above ratio of $\tau_{p=1}$ for the same initial configuration. Even for this case, however, there is a difference in the kinetic pathway between FPD and BD chains, as shown in Fig. 2(a). The difference is much more significant for the collapsing from the compact SP state, which is decelerated by HIs (squeezing effects). This effect is even opposite from that in $\tau_{p=1}$. Thus, we may say that the difference in the CGT kinetics between FPD and BD polymers (particularly, from SP to P) is due to the change of a transition path under the influence of intersegment attractive interactions, which tends to trap a polymer in metastable configurations, and not simply due to hydrodynamic renormalization of polymer dynamics.

Figure 3 plots the total potential energy per particle against R_g of the collapsing polymer. For $R_g^i/R_g^\theta = 1.66$ [Fig. 3(a)], the potential energy of the polymer with the same R_g is always higher for FPD than for BD. This indicates that with HIs, the polymer can collapse more smoothly while avoiding direct contacts and the resulting trapping in local energy minima. On the other hand, the
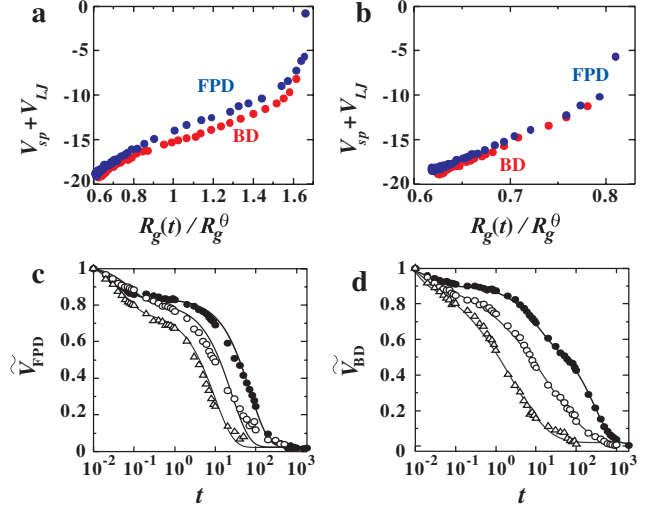

FIG. 3 (color online). Variation of $V_{sp} + V_{LJ}$ per particle during the CGT for $R_g^i/R_g^\theta = 1.66$ (a) and $R_g^i/R_g^\theta = 0.81$ (b). Temporal changes of the scaled total potential energy for FPD (c) and BD (d) for $R_g^i/R_g^\theta = 1.66$ (closed circles), $R_g^i/R_g^\theta = 1.03$ (open circles), and $R_g^i/R_g^\theta = 0.69$ (open triangles). The data in (a)–(d) were averaged over seven runs.

potential energy is only slightly higher for FPD than for BD for $R_g^i/R_g^\theta = 0.81$ [Fig. 3(b)]. This reflects the fact that the configuration of the collapsing polymer is similar between them [see the inset of Fig. 1(c)] but direct contacts are less for FPD due to HIs.

Each curve in the case of $R_g^i/R_g^\theta = 1.66$ has clear kinks [see Fig. 3(a)], suggesting that the CGT has more than two modes. Figure 3(c) shows the temporal change in the scaled total potential energy for several quenches for FPD. For larger R_g^i, it takes a longer time to reach the final globule state. The temporal change in the scaled potential energy can be fitted by a sum of two exponential decays: $\tilde{V}_{FPD}(t) = Ae^{-t/\tau_{sp}} + (1 - A)e^{-t/\tau_g}$. In the early stage, each spring shrinks due to interparticle attractions. τ_{sp} represents the fast mode stemming from this rather rapid local process. Thus, the configurational relaxation associated with the CGT can be described by the slow relaxation mode for all cases. Interestingly, the sausagelike state smoothly changes to its shrunken state even for $R_g^i/R_g^\theta > 1$ [see Fig. 1(a)]; in other words, it is just a transient state of one smooth shrinking process into the final globule state (τ_g mode).

Figure 3(d) shows the temporal change in the scaled total potential energy during CGTs for BD. In contrast to FPD, the curves are fitted by $\tilde{V}_{BD}(t) = Ae^{-t/\tau_{sp}} + Be^{-(t/\tau_c)^\beta} + (1 - A - B)e^{-t/\tau_s}$ for $R_g^i \geq R_g^\theta$ and $\tilde{V}_{BD}(t) = Ae^{-t/\tau_{sp}} + Be^{-(t/\tau_c)^\beta}$ for $R_g^i < R_g^\theta$. Note that both functions contain a stretched exponential decay mode. For $R_g^i \geq R_g^\theta$, besides the fast spring shrinking process, the CGT of BD is described by two-step decay, as shown in Fig. 1(a): the formation of clusters around both ends of the chain and their growth while absorbing the slack polymer between
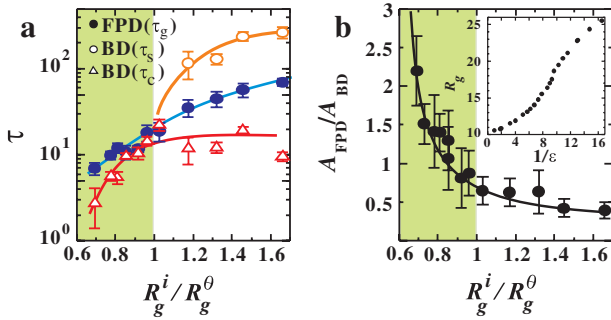
FIG. 4 (color online). Dependences of (a) the relaxation times and (b) A_{FPD}/A_{BD} on R_g^i/R_g^θ. Curves are to guide the eye. The inset shows the ϵ dependence of R_g. The error bars represent the dispersion of the data for seven independent runs.

them. τ_c and τ_s represent the time scales of the former (fast) and the latter (slow) process, respectively. For $R_g^i < R_g^\theta$, on the other hand, only one globular state is formed since most of the particles are already close to each other. Accordingly, the slow collapsing mode (τ_s mode) is not observed for BD, as can also be seen in Fig. 1(c). The stretching exponent β for each process scatters by ± 0.2 even for simulation runs starting from the same configuration. This suggests that the scatter of β reflects the statistical fluctuations of the structure of a local cluster formed in the shrinking process, which is one of many local energy minimum configurations. The cluster formation is a consequence of random trapping, which makes the escape process stochastic and results in the scatter of β.

Figure 4(a) summarizes the dependence of τ_g, τ_c, and τ_s on R_g^i. For both FPD and BD, the slow modes become slower with increasing R_g^i. When $R_g^i > R_g^\theta$, however, τ_c characterizing the cluster formation process is almost independent of R_g^i, reflecting the local nature of cluster formation. Thus, we can say that only the modes associated with the global configurational change of a polymer depend upon R_g^i. The fact that $\tau_s > \tau_g$ when $R_g^i \gtrsim R_g^\theta$ and $\tau_g > \tau_c$ when $R_g^i < R_g^\theta$ [Fig. 4(a)] indicates that a crossover in the global shrinking dynamics between BD and FPD polymers occurs around $R_g^i/R_g^\theta \cong 1$. To see this more clearly, we introduced a parameter characterizing the dynamics as $A = \int_0^\tau (R_g(t) - R_g^f)dt$, where τ is the time when the system reaches the final collapsed state. This parameter is quite robust against fluctuations of R_g. Figure 4(b) plots the ratio of A for FPD and BD, A_{FPD}/A_{BD}, as a function of R_g^i/R_g^θ. We can see a distinct crossover of the dynamics between FPD and BD around $R_g^i/R_g^\theta = 1$, where $A_{FPD} \cong A_{BD}$.

To summarize, we found that HIs accelerate collapsing for a quench from above θ point, whereas they decelerate collapsing for a quench from below θ point. We believe that the roles of HIs in the chain collapsing transition crucially depend upon the initial enhancement of anisotropy of a polymer configuration. In a swollen state, an instantaneous configuration of a polymer is elliptic [3,4], i.e., anisotropic. This anisotropy is further enhanced by the shrinking process. The resulting directional momentum flow leads to smooth one-step collapsing without being trapped in local minima. When the initial temperature is below θ point, the initial polymer configuration is nearly spherical. Thus, the flow produced by shrinking of a polymer has a radial (spherical) symmetry. This hydrodynamic squeezing effects, which are intrinsically of many-body nature, cause extra friction against polymer shrinking, and thus slow down the collapsing transition.

Finally, we mention that the deceleration of the collapsing due to HIs, or the avoidance of direct contacts between particles, may play a crucial role in preventing a protein from being trapped in local energy minima and the resulting successful protein folding from a molten to the native state. The hydrodynamic squeezing effect may give extra time for the protein to search for its global minimum configuration while avoiding direct contacts between segments. Momentum conservation may open up a new kinetic pathway to the collapsing transition of polymers, and also to the folding of proteins.

*tanaka@iis.u-tokyo.ac.jp
[1] E. D. Siggia, Phys. Rev. A **20**, 595 (1979).
[2] H. Tanaka, J. Phys. Condens. Matter **12**, R207 (2000).
[3] M. Doi and S. F. Edwards, *The Theory of Polymer Dynamics* (Clarendon, Oxford, 1986).
[4] P. G. de Gennes, *Scaling Concepts in Polymer Physics* (Cornell University, New York, 1979).
[5] S.-T. Sun *et al.*, J. Chem. Phys. **73**, 5971 (1980).
[6] P. G. de Gennes, J. Phys. (Paris), Lett. **46**, L639 (1985).
[7] E. Pitard, Eur. Phys. J. B **7**, 665 (1999).
[8] Y. A. Kuznetsov *et al.*, J. Chem. Phys. **104**, 3338 (1996).
[9] G. E. Crooks *et al.*, Phys. Rev. E **60**, 4559 (1999).
[10] R. Chang and A. Yethiraj, J. Chem. Phys. **114**, 7688 (2001).
[11] N. Kikuchi *et al.*, Eur. Phys. J. E **9**, 63 (2002); Phys. Rev. E **71**, 061804 (2005).
[12] C. F. Abrams *et al.*, Europhys. Lett. **59**, 391 (2002); J. M. Polson and N. E. Moore, J. Chem. Phys. **122**, 024905 (2005); S. H. Lee and R. Kapral, J. Chem. Phys. **124**, 214901 (2006).
[13] T. Uzawa *et al.*, J. Mol. Biol. **357**, 997 (2006).
[14] H. Tanaka, J. Phys. Condens. Matter **17**, S2795 (2005).
[15] H. Tanaka and T. Araki, Chem. Eng. Sci. **61**, 2108 (2006).
[16] B. Dünweg and K. Kremer, J. Chem. Phys. **99**, 6983 (1993).
[17] D.-J. Yang and Y.-H. Lin, Polymer **44**, 2807 (2003).
[18] K. Mussawisade *et al.*, J. Chem. Phys. **123**, 144905 (2005).
[19] H. Tanaka and T. Araki, Phys. Rev. Lett. **85**, 1338 (2000).
[20] The change in the spring length is less than 6%.
[21] A. Byrne *et al.*, J. Chem. Phys. **102**, 573 (1995).